Radiation Dose Distribution Measurements of Kilo-Voltage Photons Using Optically Stimulated Luminescence Detectors (OSLs) in Radiological Procedures

Syed Mansoor Naqvi[1,2], Zaheer Uddin[2,*], Zafar Sajjad[1], Imran Ahmed Siddiqui[2] and Amjad Hussan[3]

[1]*Department of Radiology, Aga Khan University, Karachi, Pakistan*

[2]*Department of Physics, University of Karachi, Karachi, 75270, Pakistan*

[3]*Department of Oncology, Aga Khan University, Karachi, Pakistan*

Abstract: OSL detectors were used for dose measurement in a solid water phantom. Two other detectors, Cobia Flex (RTI Electronics) and PTW-Diados were also used to verify the measurements. Radiation doses were measured for a wide range of radiographic techniques and set of parameters from very low (1 mAs, 55 kV) to very high (140 mAs, 120 kV) exposures. Multiple x-ray units were used to ensure that the measured doses are independent of x-ray units and are dependent on the specified radiographic parameters. Measurements were performed at the standard medical radiographic imaging Source-to-Image-Distances (SID) of 100 cm and 180 cm. all the x-ray beams were collimated to produce a 20 cm × 20 cm field size.

We measured the radiation doses at different depths and estimated entrance surface doses during common radiological procedures. Measured doses fall exponentially with depths at all energies and exposures. A nonlinear relation is clearly evident between the dose and the x-ray beam energy. The measurements also show that the radiation dose is directly proportional to the exposure. Entrance Surface Doses (ESD) were also measured and found to be as low as 0.119 mGy±0.020 (0.092-0.141) for extremities to as high as 13.083 mGy±3.988(8.246-17.560) to the Spine and Abdomen. ESDs for the chest x-ray were measured to be 0.158 mGy±0.074(0.034-0.275).

Keywords: Radiation dose distribution, OSL, depth doses, entrance surface dose.

INTRODUCTION

The number of diagnostic radiological examinations using kilovoltage photons has increased significantly during last few years. Although the effective dose is relatively low, nevertheless, due to the stochastic nature of radiation effects, it should be given consideration as it increases the probability of occurrence of cancer [1].

Recent advances in the imaging technology are striving towards decreasing the radiation doses while improving image quality [2]. Effective dose indicates the relative whole-body dose for a specific exam and imaging modality, and not the dose for a patient. Organ doses measures through phantoms provide direct mechanism to estimate doses for patients undergoing radiological procedures [3]. Several computer software models are available to calculate the effective doses [4].

Radiographic x-ray beam radiation dose measurements has different requirements and along with challenges as compared to the high energy megavoltage x-ray beams [5]. In the first place, as most detectors have a relatively large depth, the rapid attenuation of dose with depth means there can be a substantial dose gradient over the measuring volume of the dosimeter. Secondly the detectors behavior is related to their construction. The photoelectric interaction effect is the major radiation interaction process for the low energy x-rays, and the photoelectric cross-section is significantly depends on the atomic number of the material. Furthermore the ionization chambers do not act as Bragg–Gray cavities in the low energy x-rays and so cavity theory is not applicable [6].

Direct measurement of the x-ray beam spectrum is a harder and cannot be easily achieved in the clinical setting [7,8]. Recently the beam quality is described in terms of the half-value layer (HVL) alongwith the kilo voltage peak (kVp) [7, 9, 10, 11]. There are several variables which are dependent on HVL and are used in reference radiation dose measurements.

Optically Stimulated Luminescence (OSL) detectors were used in this study. These are becoming common for radiation dose measurements mainly for occupational exposure measurements and *in vivo* dosimetry [12, 13]. Aluminium oxide, Al_2O_3, is the most common material used to construct OSL detectors.

*Address correspondence to this author at the Department of Physics, University of Karachi, Karachi, 75270, Pakistan;
E-mail: zaheer103@yahoo.com

Table 1:

Detector	Useful Energy Range	Useful dose range	Accuracy
Cobia Flex (solid state semiconductor)	38 – 155 kVp	60 nGy – 1700 Gy	±5 %
DIADOS diagnostic detector [T60004] (solid state semiconductor)	50 - 150 keV	-	±5 %
nanoDots™ (Optically Stimulated Luminescence)	From 5 keV to 20 MeV	10 µGy to >100 Gy	± 10% with standard nanoDot™, ± 5% with screened nanoDot™

Table 2:

Phantom	Manufacturer	Mass density	Effective charge to mass (effective Z/A)	Electron density (relative to water)
RW3 Slab Phantom, Type 29672	PTW	1.045 g/cm^3	0.536	1.012

OSL detectors are fairly small in size. Al_2O_3 based OSls are 3.5 more sensitive for 125 kV as compared to 6 MV x-ray beam [14].

The OSL detectors can achieve the high degree of accuracy required for medical applications (reproducibility (< 2%)) and has a number of advantages over current methodologies such as a wide dynamic range (0.01 mGy to 15 Gy) and negligible energy, angle, dose rate, and temperature dependence.

A mechanism is needed for the determination of radiation doses received by the patients during routine radiological exams with the standard radiographic techniques and at various depths. Considering the limitation of current methodologies, the present study includes a detailed survey of the radiation doses for a wide range of the radiological exams with the standard radiographic technique factors (mAs, kV, SID) used. Using a solid water phantom, appropriate detectors and a scanning system [7, 15, 16, 17, 18] a complete set of dosimetric data in air and in solid water phantom (percent depth doses and profiles) for a kilovoltage x-rays was acquired. This study will also help in estimating organ doses by correlating the doses at different depths in phantom with the organ sites in human body.

METHOD & MATERIALS

A solid water phantom (RW3 manufacturer) is used for measurements to simulate the human body. Radiation doses were measured using the three detectors, namely: Cobia Flex (RTI Electronics,), PTW-Diados (PTW) and OSL (Landauer®). Table **1** shows the specification of the detectors used in the study.

Solid water phantom was used to simulate the patient (Table **2**).

The Super flab bolus (density 1.03 g/cc) was used to eliminate the air gap during exposure when detectors were placed between the solid water phantom sheets.

The radiation doses were measured for a large variety radiographic techniques and set of parameters from very low (1 mAs, 55 kV) to very high (140 mAs, 120 kV) exposures. Multiple x-ray units were used and it was ensured that they are producing the similar radiation output and certify that the measured doses are independent of x-ray units and are dependent on the specified radiographic parameters. Another advantage of using multiple units was to reduce heat burden which is considered as the cause of reducing the system's life so it is important to distribute the exposure over multiple x-ray machines. Table **3** lists the x-ray units used in this work.

Solid water phantom (RW3 Slab Phantom, Type 29672, PTW) with total thickness of 20 cm was used. The radiation doses were measured at surface (0 cm), 1cm, 5 cm, 10 cm, 15 cm and 20 cm depths. Intervals between exposures were given and the minimum time interval used was around the time required for the anode to stop rotating (from 3 – 4 min).

The standard medical radiographic imaging Source-to-Image-Distances (SID) of 100 cm and 180 cm were used. X-ray beams were collimated to form a 20 cm x 20 cm field size (see Figure **1A**)

Three sets of reading were taken with each detector at every set of radiographic exposure at various depths. Figure **1** shows the experimental setup:

Table 3:

Sr. #	Description	Max. mA	Max. kV	Location[a]
1	X-ray Generator, ATC-725 DEL USA.	630	150	Room-1
2	X-ray Generator, UD-150L-30E, Shimadzu.	630	150	Room-2
3	X-ray Generator, UD-150L-30E, Shimadzu.	630	150	Room-3
4	X-ray Generator, ATC-725, CPI CANADA.	630	150	Room-4
5	X-ray Generator ,UD150L-40E, Shimadzu.	630	150	Room-5
6	X-ray Generator, UD150L-40E, Shimadzu.	630	150	Room-6

[a]Department of radiology, Aga Khan University, Karachi Pakistan.
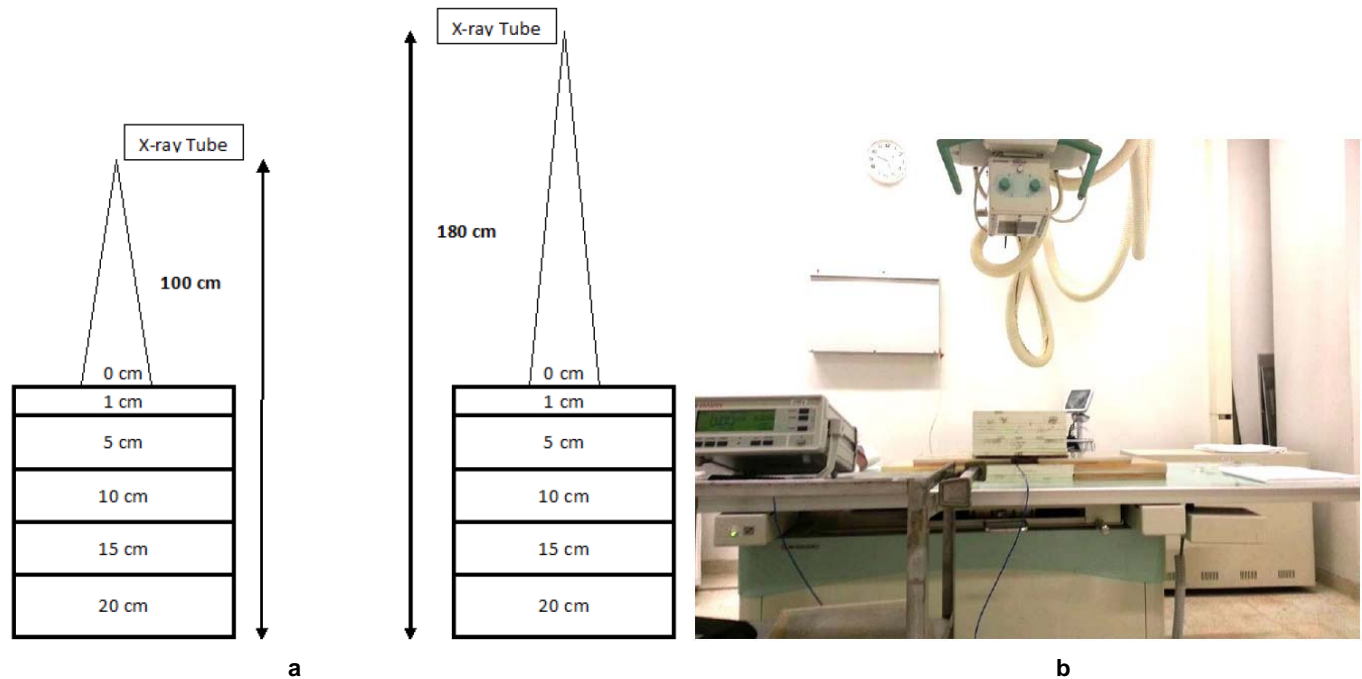
Figure 1: a: Schematic diagram showing stack of solid water phantom sheets and SID. **b:** Experimental setup.

RESULT

The results were used to evaluate the relationship between the radiation absorbed dose and the controls which are the depths, the beam energy (kV) and the exposure (mAs). Figures **2-21** shows the dependence of dose on energy and exposure at different depths, energy and depths at different exposures and exposure and depths at different energies respectively.

Figures **2** and **3** shows the doses at 100 cm SID and Figures **11-14** represent the doses at 180 cm SID. Doses measured at both SIDs show the same behavior that is the dose decreases exponentially with depths at all energies and exposures.

Figures **4**, **5** and **6** represent doses at different exposures at various depths and energies at 100 cm SID. Similarly Figures **15**, **16** and **17** show the doses at 180 cm SID, the behavior is again same for both SID

values; a linear relationship is observed for small values of mAs. For higher values of mAs, nonlinear behavior is observed.

Similar measurements are shown in Figures **7** and **18** representing radiation doses absorbed in the skin. The behavior is dependent on mAs values.

Figures **8-11** and **19-21** are plots showing doses at 100 cm and 180 cm SIDs respectively. The measurements show that the radiation dose is directly proportional to the exposure for each depth and x-ray energies.

DISCUSSION

Nonlinear behavior of absorbed dose is observed as a function of energy for different depths for higher mAs values. At lower energies the only interactions are photoelectric but at higher energies the Compton back
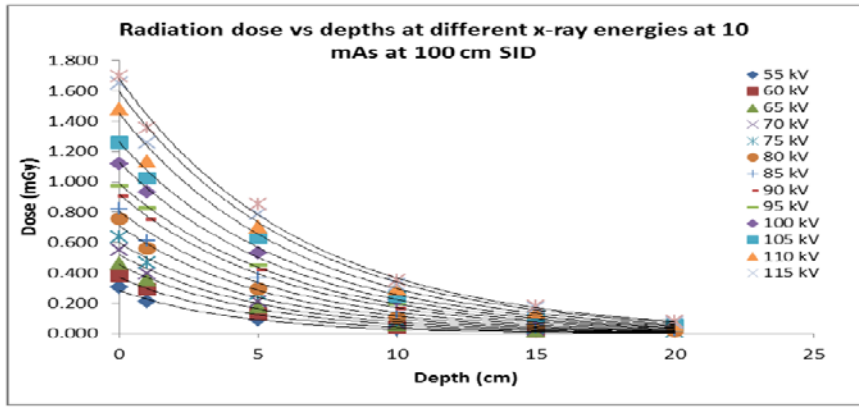
Figure 2: Radiation dose vs depths at different x-ray energies at 10 mAs at 100 cm SID.
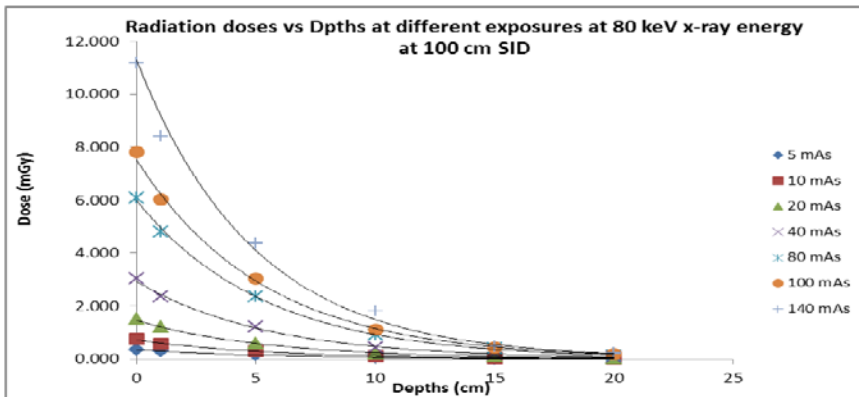
Figure 3: Radiation doses vs Depths at different exposures at 80 keV x-ray energy at 100 cm SID.
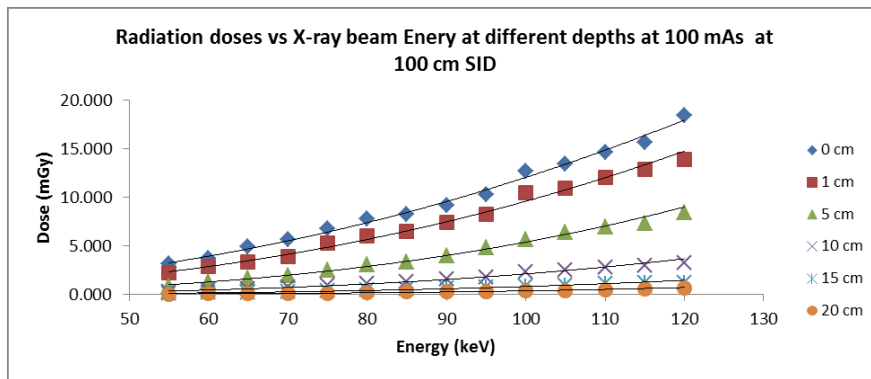
Figure 4: Radiation doses vs X-ray beam Enery at different depths at 100 mAs at 100 cm SID.
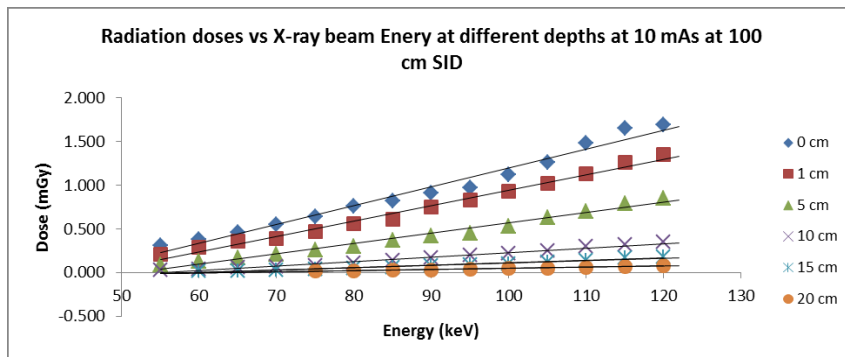
Figure 5: Radiation doses vs X-ray beam Enery at different depths at 10 mAs at 100 cm SID.
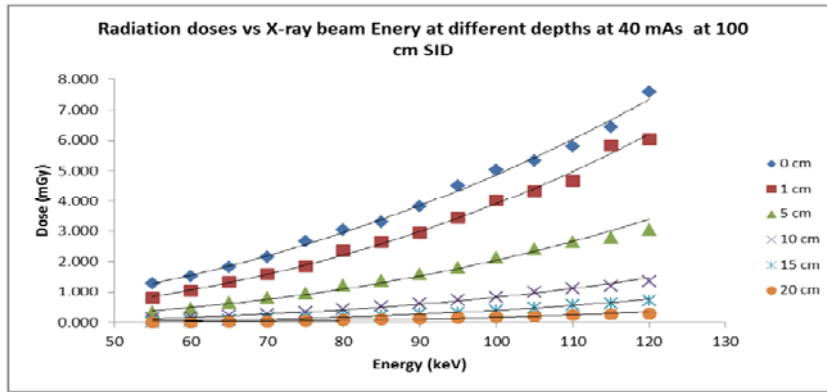
Figure 6: Radiation doses vs X-ray beam Enery at different depths at 40 mAs at 100 cm SID.
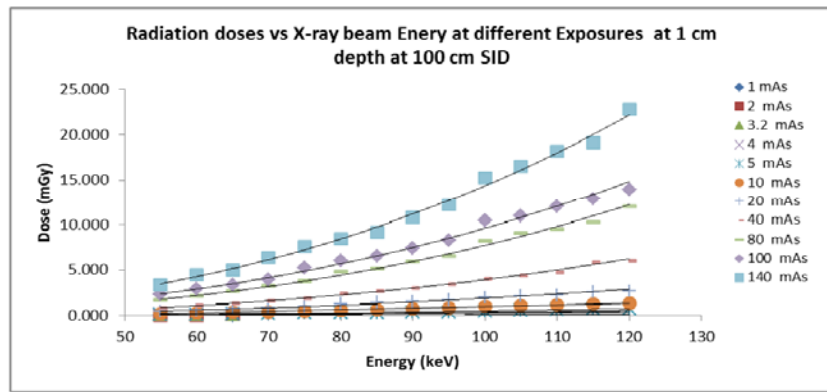
Figure 7: Radiation doses vs X-ray beam Enery at different Exposures at 1 cm depth at 100 cm SID.
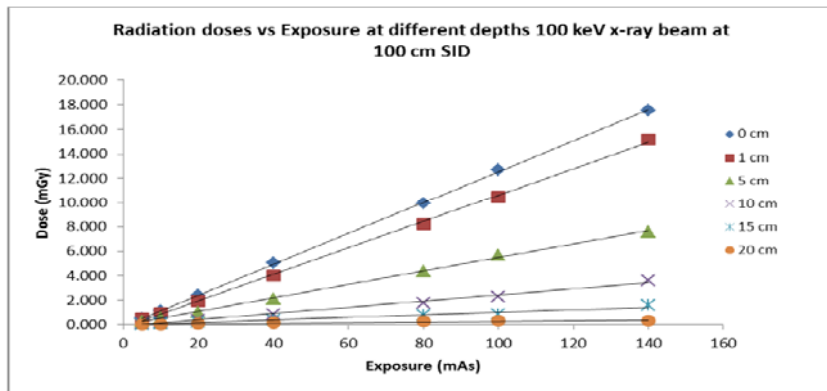
Figure 8: Radiation doses vs Exposure at different depths 100 keV x-ray beam at 100 cm SID.
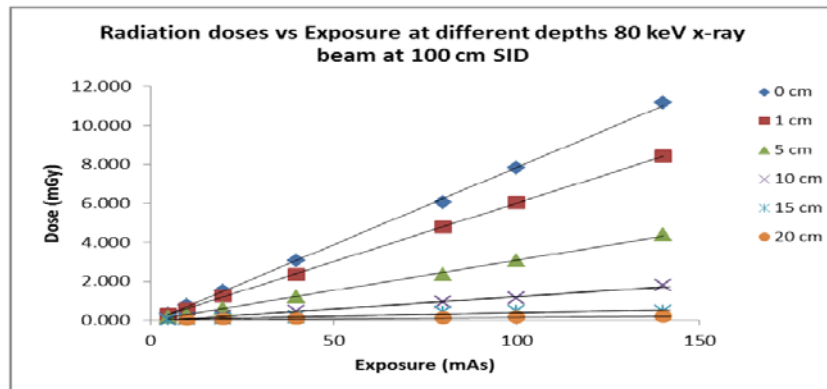
Figure 9: Radiation doses vs Exposure at different depths 80 keV x-ray beam at 100 cm SID.
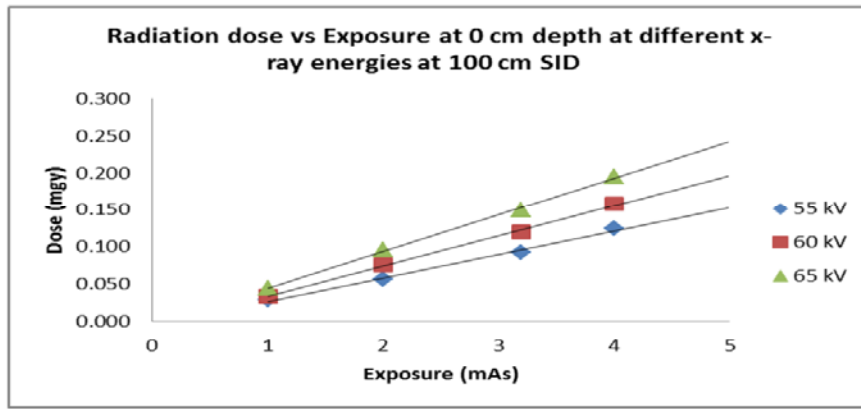
a
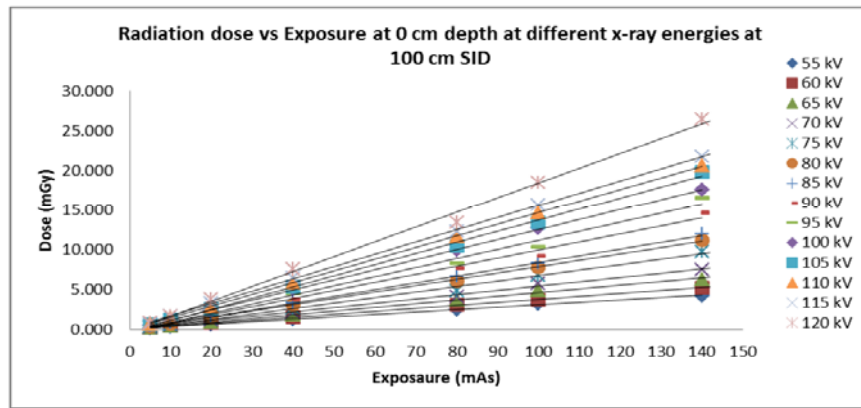
b

Figure 10: a: Radiation dose vs Exposure at 0 cm depth at different x-ray energies at 100 cm SID. **b:** Radiation dose vs Exposure at 0 cm depth at different x-ray energies at 100 cm SID.
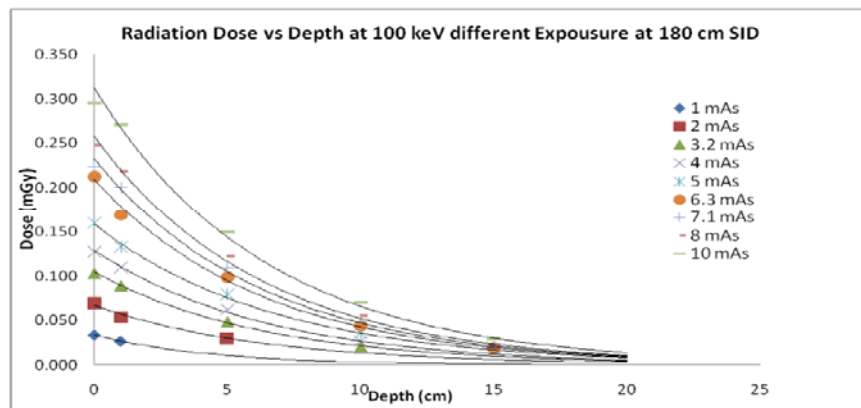
Figure 11: Radiation Dose vs Depth at 100 keV different Expousure at 180 cm SID.

scattered radiation also contributes (Figures **4** and **15**) whereas the relation between the dose and the exposure is linear, independent of depths.

The doses appeared to decrease exponentially with the depths for both energy and the exposure. This is related to the beam penetrability which is measured in HVL. In this study, we assumed that 1 HVL is equivalent to 5 cm of water. A 20-cm thick body section consists of 4 HVLs. At the exit surface, the exposure is

a small fraction of the entrance surface exposure. This clearly demonstrates the exponential behavior.

OSL nanoDot detectors are used to measure the doses which showed significant agreement(coefficient of correlation is 0.998) with the other two reference detectors, the Cobia Flex and the DIADOS from PTW. The doses measured at various depths with 0 cm corresponding to the Entrance Surface Dose, dose at 1 cm depth corresponds to the skin doses and doses at
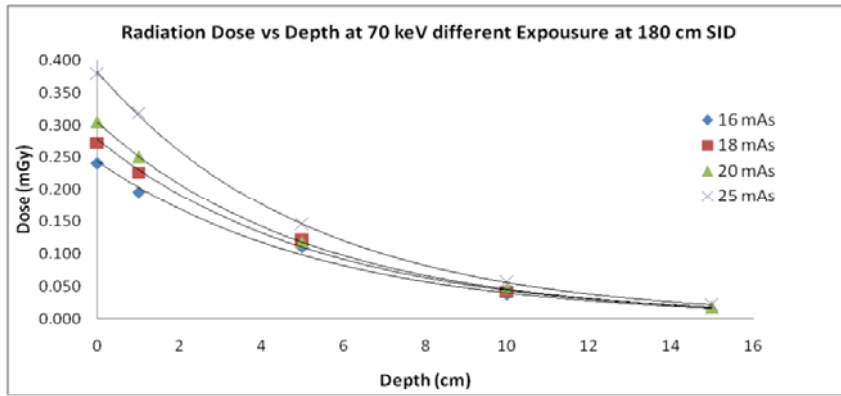
Figure 12: Radiation Dose vs Depth at 70 keV different Expousure at 180 cm SID.
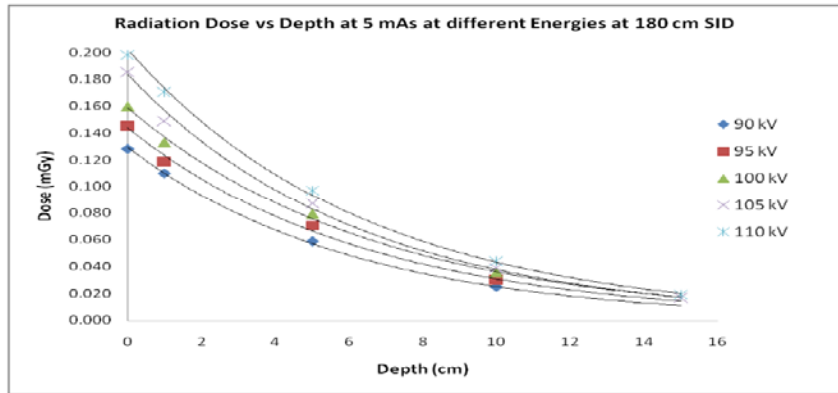
Figure 13: Radiation Dose vs Depth at 5 mAs at different Energies at 180 cm SID.
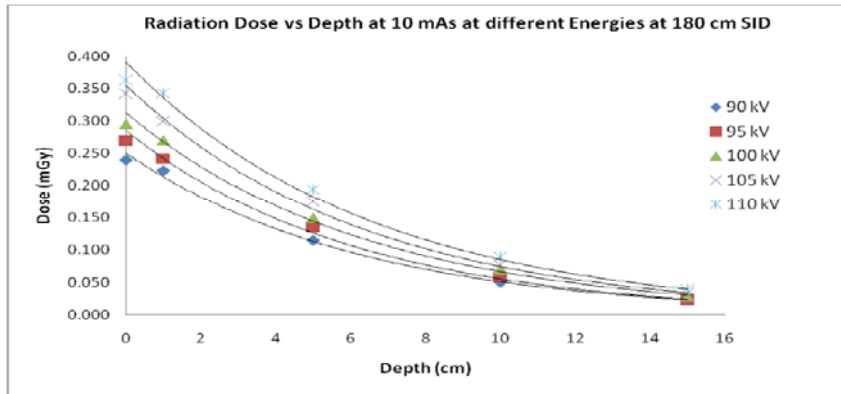
Figure 14: Radiation Dose vs Depth at 10 mAs at different Energies at 180 cm SID.
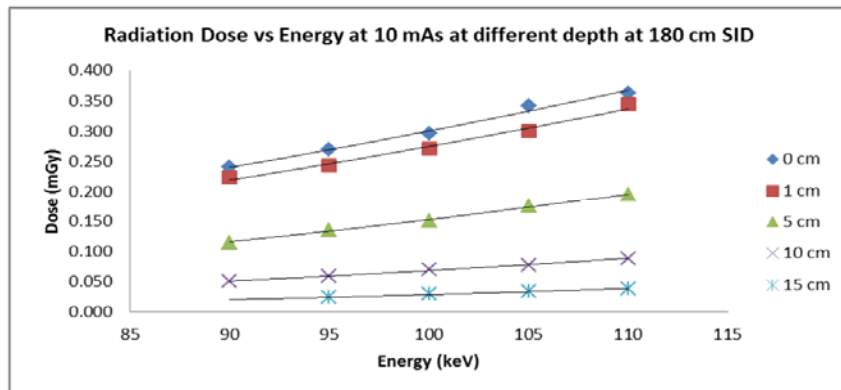
Figure 15: Radiation Dose vs Energy at 10 mAs at different depth at 180 cm SID.
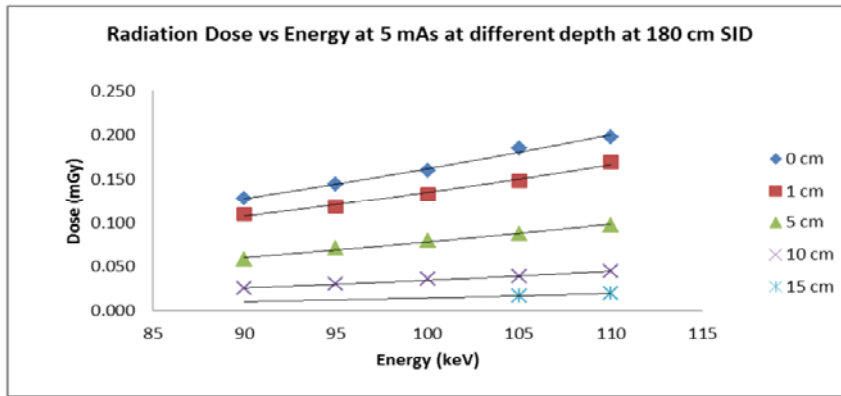
Figure 16: Radiation Dose vs Energy at 5 mAs at different depth at 180 cm SID.
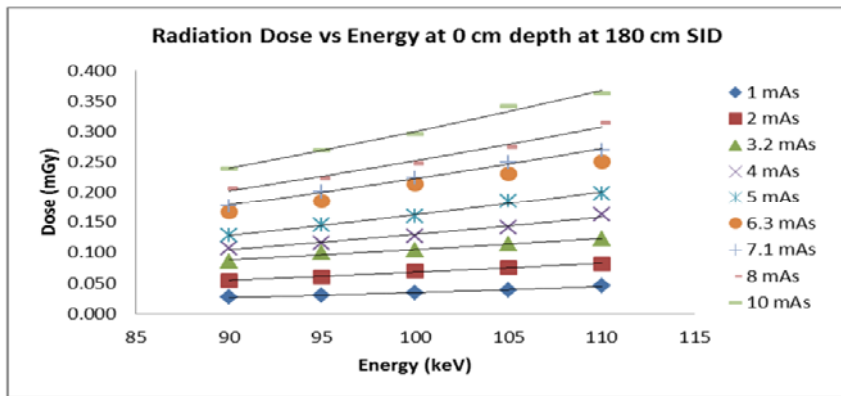
Figure 17: Radiation Dose vs Energy at 0 cm depth at 180 cm SID.
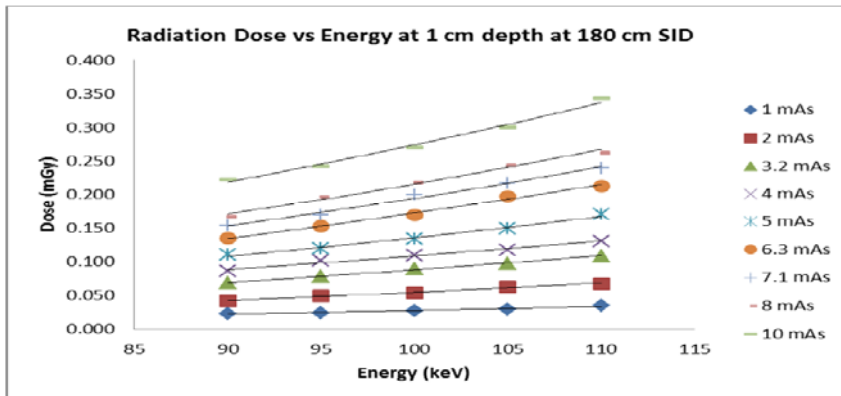
Figure 18: Radiation Dose vs Energy at 1 cm depth at 180 cm SID.
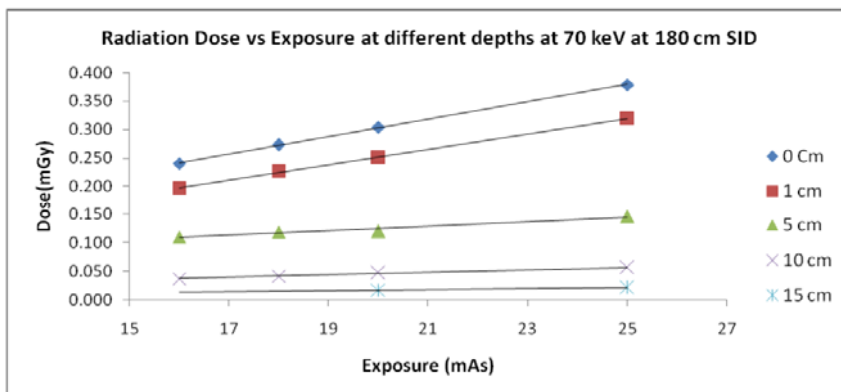
Figure 19: Radiation Dose vs Exposure at different depths at 70 keV at 180 cm SID.
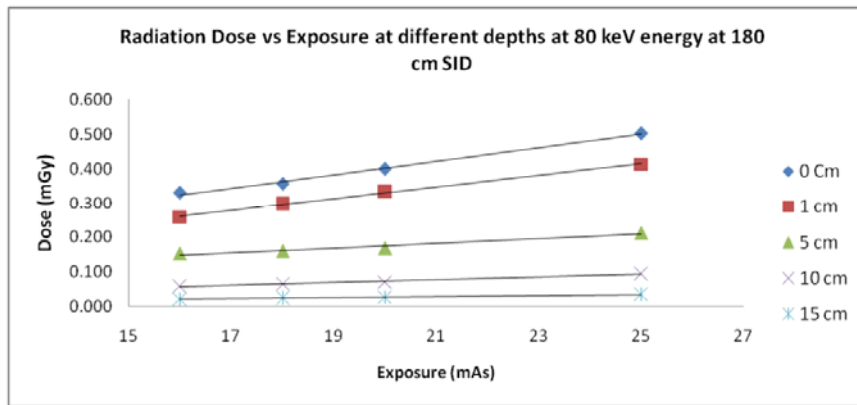
Figure 20: Radiation Dose vs Exposure at different depths at 80 keV energy at 180 cm SID.
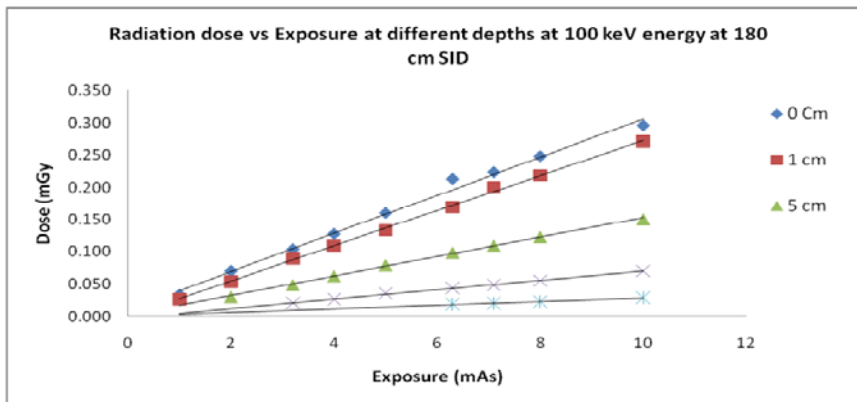
Figure 21: Radiation dose vs Exposure at different depths at 100 keV energy at 180 cm SID.

20 cm depths to the doses resulting from the exit exposure.

The results are useful as they can provide estimation of radiation doses to particular organs at different depth for example if chest x-ray is performed, then it can be estimated that how much dose the heart or lung would have received using the anatomical location of the organs and correlating it with the Figures **11** and **13**.

The effective dose is not pertinent to a specific subject but is an average estimate of dose for a reference subject in a given exposure situation. It is dependent on the radiation sensitivity of the biological tissues, the imaging technique and protocols. At present, effective dose is the only measure available to work out the overall potential biological detriment across various types of radiation exposure [19, 20]. Due to the difference in equipment, the procedures protocols and radiographic technique used, the effective doses differ for the same radiological procedure even within institutions [21]. To avoid this problem, we used 6 different units with similar specification, duly calibrated and well maintained.

In radiographic examinations, the x-ray beam irradiates patient's body. The region that receives highest exposure is the entrance surface. Table **4** shows the entrance surface doses measured using the solid water phantom and the OSL detectors. Entrance surface doses estimated in this work matches with the values estimated by other research groups as shown in Table **4**.

The limitation is the lower limit of detection as the doses below 0.016 mSv cannot be measured through nanoDots. This restricts to measure the radiation doses at depth 15 cm and more with help of the OSL detectors.

CONCLUSION

The radiation depth doses are dependent on the radiographic technique and the tissue thickness. the doses decrease exponentially with the depths at particular energies and x-ray beam intensities whereas increase non linearly with the energy and linearly with the exposure at particular depths respectively. Secondly, the OSL nanoDots are good alternative for radiation dosimetry during radiological procedures. The

Table 4: Entrance Surface Doses Measured Using the Solid Water Phantom and the OSL Detectors for Common Radiographic Exams

Procedures	Serbia and Muntenegru [22]	UK [23]	Portugal [24]	Italy [25]	Slovenia [24]	Romania [24]	Greece [24]	DRL [26]	This work
Cervical spine AP	1.3	-	2.91 (0.4-14)	-	-	-	-	-	0.307 ± 0.056 (0.218 - 0.400)
Cervical spine LAT	1.0	-	-	-	-	-	-	-	0.307 ± 0.056 (0.218 - 0.400)
Pelvis AP	2.0	4.4 (1.0-16.0)	-	7.77 (1.2-21.3)	3.8 (0.8-7.6)	13.2 (1.9-35)	12.5 ± 1.95	10	5.933 ± 2.485 (2.141 - 10.479)
Thoracic spine AP	1.5	4.7 (1.3 -18.0)	9.91 (2.3 - 16)	-	4.19 (0.9 - 7.4)	11.2 (2.0 - 41)	8.25 ± 4.62	7	5.933 ± 2.485 (2.141 - 10.479)
Lumbal spine AP	2.8	6.1 (1.4 - 31.0)	5.95 (1.4 - 23.2)	8.9 (0.6 - 42.6)	6.9 (0.7 - 26.9)	17.6 (2.0 - 71)	18.9 ± 6.76	10	5.933 ± 2.485 (2.141 - 10.479)
Lumbal spine LAT	4.4	16.0 (3.9 -75)	-	26.7 (1.2 86.7)	16.8 (2.3 - 60)	42.0 (4.4 162)	44.9 ± 22.9	30	13.083 ± 3.988 (8.246 - 17.560)
Chest PA	0.4	0.16 (0.01 - 0.10)	0.31 (0.06 - 3.2)	0.57 (0.1 - 4-13)	0.23 (0.08 - 0.4)	1.7 (0.3 - 6.0)	0.69 ± 0.40	0.3	0.158 ± 0.074 (0.034 - 0.275)
Chest LAT	0.3	0.57 (0.11 - 2.6)	-	1.88 (0.2 - 13.7)	0.67	4.2 (0.7 - 13)	2.94 ± 1.57	-	0.288 ± 0.036 (0.241 - 0.330)
Skull PA	1.15	3.0 (0.5 - 10)	-	7.38 (2.29 - 21.8)	-	11 (1.0 - 31)	3.5 ± 1.9	-	1.159 ± 0.345 (0.824 - 1.512)
Skull LAT	0.9	1.5 (0.56 - 4.43)	7.27 (0.49 - 21)	4.15 (1.21 - 15.9)	-	9.4 (1.2 - 28)	2.7 ± 1.5	-	0.307 ± 0.056 (0.218 - 0.400)

advantage with the nanoDots is the smaller size and sensitivity which contributes in the effective use of them as standard dosimeters.

REFERENCES

[1] National Research Council. Health risks from exposure to low levels of ionizing radiation: BEIR VII phase 2. Washington, DC: National Academies Press 2006.

[2] McCollough CH. CT dose: how to measure, how to reduce. Health Phys 2008; 95: 508-17.
http://dx.doi.org/10.1097/01.HP.0000326343.35884.03

[3] Huda W, Sandison GA. The use of the effective dose equivalent, HE, as a risk parameter in computed tomography. Br J Radiol 1986; 59: 1236-1238.
http://dx.doi.org/10.1259/0007-1285-59-708-1236

[4] McCollough CH, Schueler BA. Calculation of effective dose. Med Phys 2000; 27: 828-837.
http://dx.doi.org/10.1118/1.598948

[5] Nahum AE. Perturbation effects in dosimetry: part 1. Kilovoltage x-rays and electrons. Phys Med Biol 1996; 41: 1531-80.
http://dx.doi.org/10.1088/0031-9155/41/9/001

[6] Ma CM, Nahum AE. Bragg–Gray theory and ion chamber dosimetry for photon beams. Phys Med Biol 1991; 36: 413-28.
http://dx.doi.org/10.1088/0031-9155/36/4/001

[7] Ma CM, Coffey CW, DeWerd LA, Liu C, Nath R, Seltzer SM, Seuntjens JP. AAPM protocol for 40–300 kV x-ray beam dosimetry in radiotherapy and radiobiology. Med Phys 2001; 28: 868-893.
http://dx.doi.org/10.1118/1.1374247

[8] Seuntjens J, Thierens H, Segaert O. A Response of coaxial Ge(Li) detectors to narrow beams of photons for stripping of x-ray bremsstrahlung spectra. Nucl Inst Methods Phys Res A 1987; 258: 127-31.

[9] Andreo P, Burns DT, Hohlfield K, Huq MS, Kanai T, Laitano F, Smyth V, Vynckier S. Absorbed dose determination in external beam radiotherapy, an international code of practice for dosimetry based on standards of absorbed dose to water Technical Report Series No 398 (Vienna: IAEA, 2000).

[10] Klevenhagen SC, Aukett RJ, Harrison RM, Moretti C, Nahum AE, Rosser KE. The IPEMB code of practice for the determination of absorbed dose for x-rays below 300 kV generating potential (0.035 mm Al–4 mm Cu HVL; 10–300 kV generating potential). Phys Med Biol 1996; 41: 2605-25.
http://dx.doi.org/10.1088/0031-9155/41/12/002

[11] Grimbergen TWM, Aalbers AHL, Mijnheer BJ, Seuntjens J, Thierens H, Van Dam J, Wittkamper FW, Zoetelief J. Dosimetry for low and medium energy x-rays: a code of practice in radiotherapy and radiobiology Technical Report 10, 1997, Netherlands Commission on Radiation Dosimetry.

[12] Akselrod MS, Btter-Jensen L, McKeever SWS. Optically stimulated luminescence and its use in medical dosimetry. Radiat Meas 2006; 41(Suppl. 1): S78-99.

[13] Yukihara EG, McKeever SWS. Optically stimulated luminescence OSL dosimetry in medicine. Phys Med Biol 2008; 53: R351-79.
http://dx.doi.org/10.1088/0031-9155/53/20/R01

[14] Reft CS. The energy dependence and dose response of a commercial optically stimulated luminescent detector for kilovoltage photon, megavoltage photon and electron, proton and carbon beams. Med Phys 2009; 36: 1690-9.
http://dx.doi.org/10.1118/1.3097283

[15] Hill, *et al.* Ionization chamber dosimetry for kilovoltage x-ray beams "An evaluation of ionization chambers for the relative

dosimetry of kilovoltage x-ray beams. Med Phys 2009; 36: 3971-81.
http://dx.doi.org/10.1118/1.3183820

[16] Li XA, Ma CM, Salhani D. Measurement of percentage depth dose and lateral beam profile for kilovoltage x-ray therapy beams. Phys Med Biol 1997; 42: 2561-68.
http://dx.doi.org/10.1088/0031-9155/42/12/019

[17] Ma CM, Li XA, Seuntjens JP. Study of dosimetry consistency for kilovoltage x-ray beams. Med Phys 1998; 25: 2376-2384.
http://dx.doi.org/10.1118/1.598448

[18] British Journal of Radiology. Central axis depth dose data for use in radiotherapy. Br J Radiol Suppl. 1996; 25.

[19] Dietze G, Harrison JD, Menzel HG. Effective dose: a flawed concept that could and should be replaced: comments on a paper by D J Brenner (Br J Radiol 2008; 81: 521-3). Br J Radiol 2009; 82: 348-50.
http://dx.doi.org/10.1259/bjr/91937653

[20] Martin CJ. Effective dose: how should it be applied to medical exposures? Br J Radiol 2007; 80: 639-47.
http://dx.doi.org/10.1259/bjr/25922439

[21] Hausleiter J, Meyer T, Hermann F, *et al.* Estimated radiation dose associated with cardiac CT angiography. JAMA 2009; 301: 500-7.
http://dx.doi.org/10.1001/jama.2009.54

[22] Ciraj O, Marković S, Košutić D. Patient Dose From Conventional Diagnostic Radiology Procedures In Serbia And Montenegro. The Journal Of Preventive Medicine 2004; 12(3-4): 26-34.

[23] Shrimpton PC, Wall BF, Jones DG. Doses to patients from routine diagnostic X-ray examinations in England. Br J Radiol 1986; 59: 749-58.
http://dx.doi.org/10.1259/0007-1285-59-704-749

[24] United Nations Scientific Committee on the Effects of Atomic Radiation: Source and Effects of Ionizing Radiation. Report to the General Assembly. United Nations. New York 2000.

[25] Padovani R, Contetnto G, Fabretto M. Patient doses and risks from diagnostic radiology in north-east Italy. Br J Radiol 1987; 60: 155-65.
http://dx.doi.org/10.1259/0007-1285-60-710-155

[26] European Commission: European Commission. European Guidelines on Quality Criteria for Diagnostic Radiographic Images, EUR 16260 EN 1996.